Crystal-Bound *vs* Surface-Bound Thiols on Nanocrystals

Michael J. Turo and Janet E. Macdonald*

Department of Chemistry, Vanderbilt Institute for Nanoscale Science and Engineering, Vanderbilt University, Nashville, Tennessee 37235, United States

ABSTRACT The use of thiol ligands as a sulfur source for nanocrystal synthesis has recently come *en vogue*, as the products are often high quality. A comparative study was performed of dodecanethiol-capped Cu_2S prepared with elemental sulfur and thiol sulfur reagents. XPS and TGA-MS provide evidence for differing binding modes of the capping thiols. Under conditions where the thiol acts only as a ligand, the capping thiols are "surface-bound" and bond to surface cations in low coordination number sites. In contrast, when thiols are used as a sulfur source, "crystal-bound" thiols result that sit in high coordination sites and are the terminal S layer of the crystal. A ^{1}H NMR study shows suppressed surface reactivity and ligand exchange with crystal-bound thiols, which could limit further application of the particles. To address the challenge and opportunity of nonlabile ligands, dodecyl-3-mercaptopropanoate, a molecule possessing both a thiol and an ester, was used as the sulfur source for the synthesis of Cu_2S and $CuInS_2$. A postsynthetic base hydrolysis cleaves the ester, leaving a carboxylate corona around the nanocrystals and rendering the particles water-soluble.

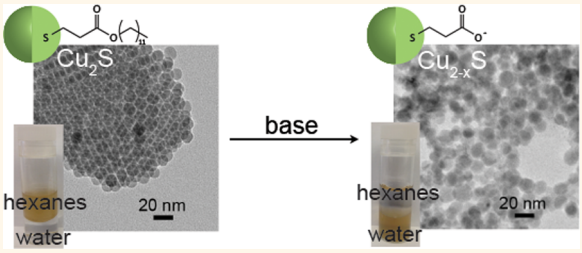

KEYWORDS: Cu_2S · $CuInS_2$ · nanocrystals · surface chemistry · water solubility

There has been considerable interest in using semiconducting nanocrystals for biomedical,[1] electronic,[2] and alternative energy applications.[3] This interest stems from the optical properties, which can be tuned by particle size *via* quantum confinement or changing the composition. Even a slight change of size, morphology, or composition of nanocrystals has a considerable effect on the optical properties including the energies of the absorption onset, fluorescence emission,[4] and surface plasmons. Thus, syntheses to monodisperse, single crystalline nanocrystals are desired. While there are many ways to synthesize nanocrystals, solution-based colloidal synthesis often yields the highest quality, most monodisperse samples, with uniform properties.[4]

Typical solution syntheses to prepare nanocrystals in organic solvents involve the chemical transformation of dissolved molecular inorganic reagents to solids. This is performed in the presence of ligands to coordinate to the nanocrystal surfaces. The ligands lower the surface energy and allow for the thermodynamically unfavorable nanocrystals to be kinetically trapped.[5] The ligands possess a long alkyl chain that provides solubility in the high-boiling organic solvents required for the synthesis and a polar head group to bind to the surface. Common head groups are phosphines, phosphine oxides, carboxylic acids, phosphonic acids, amines, or thiols.

Thiols are in a special category of ligands because they can concomitantly act as the sulfur source in syntheses of metal sulfide nanocrystals.[6−20] At high temperatures, thiols decompose on the metal centers to yield the metal sulfide and an alkene.[6] At the termination of the reaction, the particles are capped with a final layer of intact thiols.

The use of thiols as a sulfur source for nanocrystal synthesis has become increasingly common as the products are often of very high quality. For example, syntheses of monodisperse, single-crystalline, shape-controlled particles of copper sulfide[6−10,21] and mixed copper sulfides[11−15] use this technique. Thiols have also been employed as a sulfur source for shelling quantum dots of CdSe with ZnS and CdS to improve fluorescence yields and reduce blinking.[17−20]

We and others have noted that copper sulfides prepared with thiol sulfur precursors are resistant to ligand exchange procedures for surface functionalization and to impart water solubility.[13,22] The inert surfaces will preclude the use of these nanocrystals in most biomedical, sensor,

* Address correspondence to janet.macdonald@vanderbilt.edu.

Received for review June 13, 2014 and accepted September 14, 2014.

Published online September 15, 2014
10.1021/nn5032164

and photocatalytic applications. In quantum dot sensitized photovoltaic devices, these tightly bound thiols would need to be removed to improve interparticle conductivity.[23]

Besides the empirical observation of poor ligand lability, here we present ^{1}H NMR, X-ray photoelectron spectroscopy (XPS), and thermogravimetric analysis–mass spectroscopy (TGA-MS) studies to provide evidence that when thiols are used as a sulfur source, the capping thiols are bound to the surface of the nanocrystals in a chemically different manner than typical ligand–surface interactions. When the only role of the thiols is as ligands, thiols are bound to cations at low coordination number surface sites, which we describe as "surface-bound" in this report (Figure 1).[24,25] The capping thiols that result from reactions where they are also the sulfur source become the terminal layer of sulfurs of the crystal. These thiols are exceptionally strongly bound because they sit in high coordination number sites. We call these "crystal-bound thiols" in this report (Figure 1).

Furthermore, we present a simple and broadly applicable method to achieve water solubility of metal sulfide nanocrystals synthesized with thiol precursors. Dodecyl-3-mercaptopropanoate (D3MP), a long-chain thiol with a midchain ester, was synthesized and used to replace 1-dodecenethiol as a ligand and sulfur source for representative syntheses of Cu_2S and $CuInS_2$ nanocrystals. The midchain ester can be readily cleaved to make otherwise immutably organic soluble particles transfer into water.

RESULTS AND DISCUSSION

Evidence for Crystal-Bound Thiols. To gather evidence for the chemical uniqueness of crystal-bound thiols, Cu_2S nanocrystals were prepared by two methods to give surfaces capped by crystal-bound and surface-bound thiols both with the chalcocite crystal structure (Supporting Information). Cu_2S nanocrystals with crystal-bound dodecanethiol (DDT) were prepared according to literature procedure by heating $Cu(acac)_2$ with dodecanethiol at 200 °C in dioctyl ether (DOE) solvent.[6,8] The single crystalline particles were 6.9 ± 0.5 nm (n = 188). Cu_2S nanocrystals with surface-bound thiols were prepared by a modified literature procedure[26] whereby $Cu(acac)_2$ was allowed to react with sulfur powder at 200 °C in oleylamine (OLAM) and oleic acid (OA) to give 6.8 ± 1.1 nm (n = 169) nanocrystals. After the reaction, the particles underwent a ligand exchange with DDT (Figure 2). The ligand exchange to DDT capping ligands was confirmed by IR spectroscopy, which showed the disappearance of the carbonyl stretch of oleic acid (Supporting Information).

NMR is a powerful technique for the determination of the interactions between ligands and nanocrystal surfaces.[25,27−30] Changes in the spectrum resulting from perturbations allow for the dynamic interactions

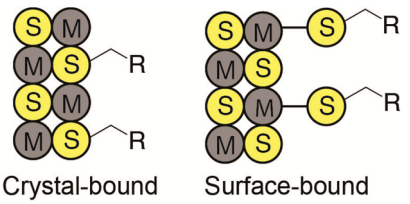

Figure 1. Two binding modes of thiol ligands on metal sulfide nanocrystals.

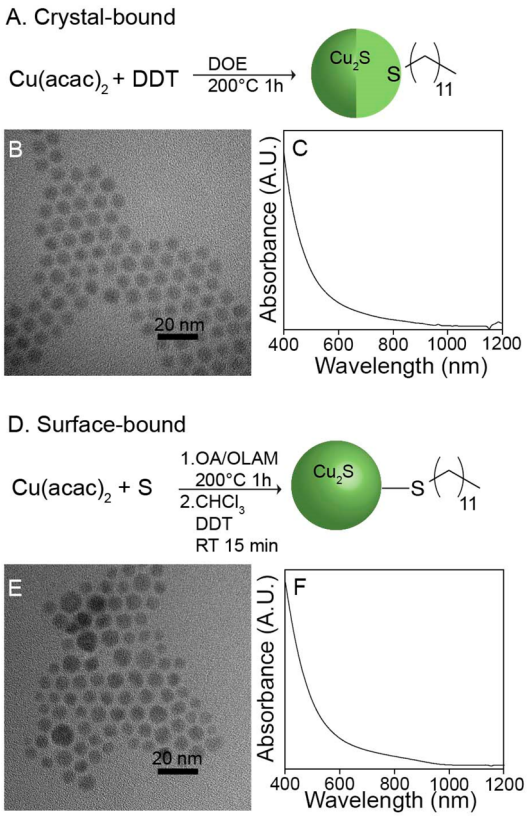

Figure 2. (A) Synthesis of Cu_2S nanocrystals with crystal-bound dodecanethiol capping ligands. (B) TEM of Cu_2S nanocrystals with crystal-bound ligands, d = 6.9 ± 0.5 nm, n = 188. (C) Absorbance spectrum of Cu_2S nanocrystals with crystal-bound ligands. (D) Synthesis of Cu_2S nanocrystals with surface-bound dodecanethiol. (E) TEM of Cu_2S nanocrystals with surface-bound ligands, d = 6.8 ± 1.1 nm, n = 169. (F) Absorbance spectrum of Cu_2S nanocrystals with surface-bound ligands.

between the ligands and the nanocrystal to be observed. The protons near the particle surface are often not observed by ^{1}H NMR due to short T_2 relaxation times,[29] but when the ligand has a suitable midchain NMR signal such as the double bond of oleic acid or oleylamine, dynamic ligand self-exchange can be identified using 2D NMR techniques.[25,27−30] DDT does not have such unsaturation, and so instead we examined the heteroexchange between the native DDT on the particle surface to D3MP (synthesis *vide infra*), which has distinctive ^{1}H NMR signals (Figure 3A) as compared to DDT.

^{1}H NMR spectra of the thiol- and sulfur-derived nanocrystals are shown in part in Figure 3 and in full

in the Supporting Information. In the regions reported in Figure 3A, there are no peaks that can be assigned to DDT; however, a small amount of 1,1-didodecyldisulfide[31] (Supporting Information) was observed in the surface-bound sample. Disulfide formation on nanocrystal surfaces has been observed previously for thiol-capped semiconductor nanocrystals[32,33] and has limited the stability of the particles in solution.[32]

To the NMR tubes containing the DDT-capped nanocrystals, 2 molar equiv of D3MP as compared to the DDT capping ligands were added. In both the crystal-bound and surface-bound samples (Figure 3), the addition of the new ligand caused the expected appearance of signals from D3MP: a triplet at 4.10 ppm, a quartet at 2.77 ppm, and a triplet 2.65 ppm, labeled γ, α, and β, respectively.

After 24 h in the ^{1}HNMR solution in the presence of D3MP and exposure to ambient light, the crystal-bound thiols on Cu_2S showed much greater chemical stability than surface-bound thiols. For crystal-bound thiol samples small peaks at 2.92 and 2.73 ppm as well as a small shoulder on the peak at 4.10 ppm were observed, which can be assigned to the formation of didodecyl 3,3′-disulfanediyldipropionate, the disulfide of two D3MP molecules (Supporting Information). The disulfide formation is known to be surface mediated.[33] This suggests that there are a small number of exposed coordination sites when crystal-bound ligands are expected. There is however no evidence that the exposed surface is a result of the native ligands dissociating from the nanocrystal surface.

In contrast to nanocrystals with crystal-bound thiols, there was evidence of mobility of the native ligands on nanocrystals with surface-bound thiols after 24 h in the ^{1}HNMR solution in the presence of D3MP and exposure to ambient light. The ^{1}H NMR showed a decrease in the concentration of free D3MP resulting from a high rate of formation of disulfides. Disulfides form more readily because of the dynamic nature of the native capping thiols. In addition to didodecyl 3,3′-disulfanediyldipropionate, there were also peaks at 2.7−2.75 ppm and offset but overlapping peaks at 2.91 ppm and at 4.10 ppm, which we assign to two additional disulfides, 1,1-didodecyldisulfide, and the mixed disulfide dodecyl 3-(dodecyldisulfanyl)-propanoate (Supporting Information). The disulfides that contain DDT units are a direct result of the removal of the native DDT bound to the nanocrystal surface. These DDT-containing disulfides are not observed in the crystal-bound case because the native ligands are nonlabile.

The sum of the ^{1}H NMR study shows that when thiols are used as the sulfur source in the synthesis of Cu_2S, the resulting capping thiols have significantly different surface chemistry than if the thiol is simply exchanged onto the surface. While surface-bound thiols are labile and prone to oxidative disulfide formation, crystal-bound thiols are nonlabile and resistant to oxidation.

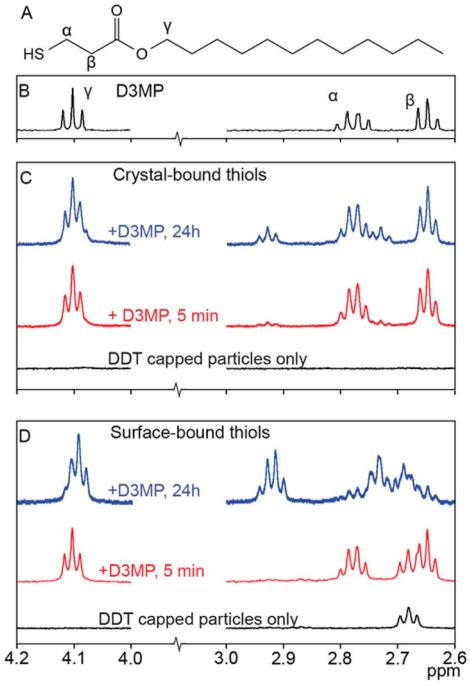

Figure 3. (A) Structure of D3MP. (B) Partial ^{1}H NMR spectrum of D3MP. (C) ^{1}H NMR spectra for Cu_2S nanocrystals with crystal-bound dodecanethiol (black), 5 min after the addition of 2 molar equiv of D3MP (red) and at 24 h after addition (blue). (D) ^{1}H NMR spectra for Cu_2S nanocrystals with surface-bound dodecanethiol (black), 5 min after the addition of 2 molar equiv of D3MP (red), and at 24 h after addition (blue).

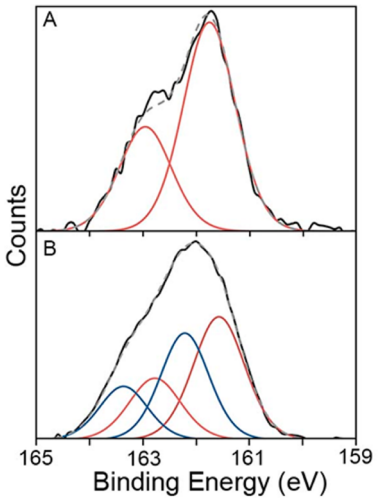

Figure 4. S 2p XPS spectra of Cu_2S nanocrystals with (A) crystal-bound DDT capping ligands and (B) surface-bound DDT capping ligands.

X-ray photoelectron spectroscopy (XPS) was employed to further identify differences in the surface chemistries between crystal-bound and surface-bound thiol ligands. The S 2p region of Cu_2S with crystal-bound DDT (Figure 4A) was compared to that of Cu_2S with surface-bound DDT (Figure 4B). Efforts were made

to minimize the exposure of the samples to air prior to analysis to prevent oxidation of the copper sulfide.[34]

For the nanocrystals with crystal-bound DDT the peak in the XPS S 2p region was best fit by one set of spin–orbital coupled peaks at 161.8 and 163.0 eV and was assigned the S in the Cu_2S crystal lattice.[34] Nanocrystals with surface-bound DDT were best fit by two sets of spin orbital couples. The lower energy set is at 161.6 and 162.8 eV and arises from the sulfur in the Cu_2S crystal lattice. A second set with a higher binding energy was fitted at 162.2 and 163.4 eV and can be attributed to thiolate bound to the surface of Cu_2S.[35] The absence of the peaks for thiolate binding to the surface of Cu_2S in the crystal-bound sample is indicative that the thiol capping ligands are not simply bound to individual surface Cu, but rather bound into higher coordination sites within the crystal lattice.

TGA-MS also points to very different surface chemistries between crystal-bound and surface-bound thiols (Figure 5 and Supporting Information). For both Cu_2S nanocrystals with surface-bound and crystal-bound thiols, there is a large mass loss between 200 and 300 °C. Mass spectrometry of the species emanated is dominated by 1-dodecene, which can be formed from alkyl migration and β-hydride elimination of the thiols on the surface.[36] Above 300 °C Cu_2S nanocrystals with crystal-bound ligands show almost no mass loss, whereas almost 20% of the mass lost for Cu_2S nanocrystals with surface-bound ligands occurs at these higher temperatures. Above 300 °C, the ion in the mass spectrometry has an *m/z* consistent with S_2, disulfide, the most abundant ion seen in mass spectrometry of gas phase sulfur from the decomposition of metal sulfides.[37,38]

After β-hydride elimination of dodecene, the remaining S on the Cu_2S surface is different for crystal-bound *vs* surface-bound thiols. Surface-bound thiols will leave sulfur in low coordination sites, which is removed at higher temperatures. Crystal-bound thiols leave sulfurs in high-coordination sites, which prevents further mass loss of the sulfur.

Water Solubility of the Copper Sulfides with Crystal-Bound Ligands. Since the robust binding mode of crystal-bound thiols makes the particles immune to ligand exchange at moderate temperatures, an alternative method is needed to impart chemical modification to the nanocrystal surface to allow water solubility. At the same time, a methodology was desired that would not greatly alter the established syntheses of the high-quality particles yielded when a long-chain thiol was the sulfur source. We chose to modify the ligand alkyl chain by adding a midchain ester, which provided protected chemical functionality. Purified D3MP was synthesized in multigram scale by using a Fischer esterification from the inexpensive reagents 3-mercaptopropionic acid (MPA) and 1-dodecanol (Figure 6A).[39]

D3MP was used instead of DDT in the synthesis of Cu_2S nanocrystals (Figure 2A *vs* 6B). The transmission

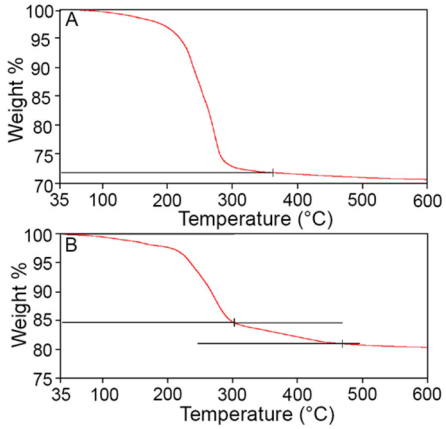

Figure 5. (A) TGA of Cu_2S nanocrystals with crystal-bound dodecanethiol. (B) TGA of Cu_2S nanocrystals with surface-bound dodecanethiol. MS traces of the emanated species are included in the Supporting Information.

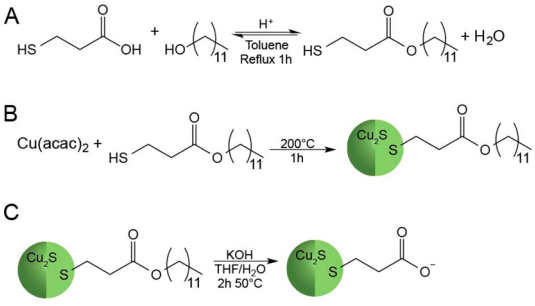

Figure 6. (A) Synthesis of dodecyl-3-mercaptopropanoate from 3-mercaptopropionic acid and 1-dodecanol. (B) Synthesis of Cu_2S using D3MP as the sulfur source. (C) Base-catalyzed hydrolysis of the D3MP-capped particles.

electron microscopy (TEM) image (Figure 7A) shows the resulting 11.9 ± 0.9 nm (n = 222) Cu_2S particles packed into a superlattice, indicating highly monodisperse particles.[4,9] The phase was confirmed to be chalcocite Cu_2S by selected area electron diffraction (SAED) (Supporting Information).

In a postsynthesis step, a base hydrolysis cleaved the midchain ester to leave the surfaces capped with a corona of carboxylates, rendering the particles water-soluble (Figure 6C). TEM revealed that the hydrolysis did not significantly change the size of the particles (Figure 7B and Supporting Information). Infrared spectroscopy confirmed the cleavage of the ligand (Figure 7C) from the D3MP ester to a deprotonated MPA carboxylate, as the ester carbonyl stretching mode at 1737 cm^{-1} was replaced with two modes at 1606 and 1402 cm^{-1}, representing the symmetric and asymmetric stretches of a carboxylate. In addition, the C–H stretching mode between 3000 and 2800 cm^{-1} decreases in intensity from the loss of the long alkyl chain.

The hydrolysis resulted in a change in the optical properties of the Cu_2S. While the initial synthesis gives an absorbance spectrum consistent with Cu_2S, a broad

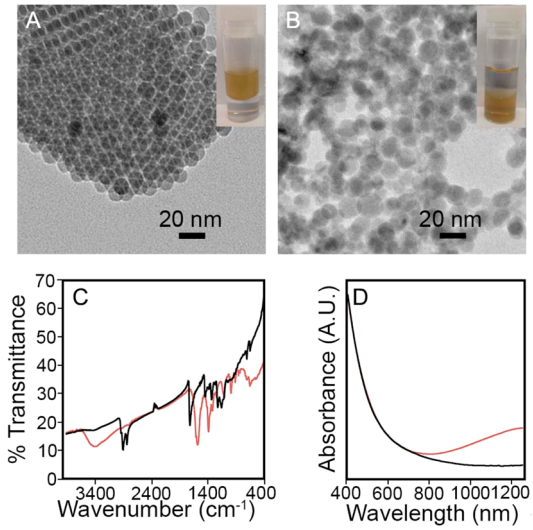

Figure 7. (A) TEM of Cu_2S synthesized using D3MP as the sulfur source, 11.9 ± 0.9 nm, n = 222. Inset is a photograph of the particles dissolved in hexanes phase above a water layer. (B) Particles after hydrolysis of the ligand, 13.0 ± 2.0 nm, n = 237. Inset is a photograph of the particles dissolved in water below a layer of hexanes. (C) Infrared spectrum of Cu_2S before (black) and after (red) hydrolysis. (D) Normalized absorbance spectra of Cu_2S before the hydrolysis dispersed in hexanes (black) and after the hydrolysis dispersed in water (red).

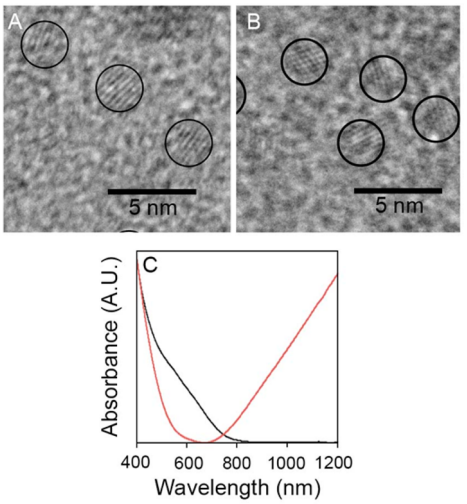

Figure 8. (A) TEM images of $CuInS_2$ synthesized using D3MP as the sulfur source, 2.41 ± 0.29 nm, n = 132 (B) and after ester hydrolysis, 2.34 ± 0.27 nm, n = 140. (C) The normalized absorbance spectra of $CuInS_2$ before the hydrolysis dispersed in hexanes (black) and after the hydrolysis dispersed in water (red).

surface plasmon resonance in the near-infrared region of the absorbance spectrum developed (Figure 7D) during the hydrolysis that is indicative of substoichiometric $Cu_{2-x}S$.[40] SAED was consistent with the substoichemetric Djurleite crystalline phase, which is closely related to chalcocite (Supporting Information). The free carrier density was determined by dissolving the water-soluble particles in anhydrous THF and collecting a spectrum into the near-IR. The larger solvent window of THF was needed in order to observe the peak of the plasmon (Supporting Information).[41] Using Drude's relationship between the bulk plasmon frequency and the carrier density, N_h, the carrier density was determined to be 3.56×10^{20} cm^{-3}, which corresponds to a stoichiometry of $Cu_{1.98}S$ (Supporting Information).

The leaching of the Cu^{2+} cations into solution is not unprecedented for crystal-bound ligands on Cu_2S nanocrystals. Previous work has shown that when dodecanethiol was used as the sulfur source in the synthesis of Cu_2S, cation exchange reactions to CdS or PbS are possible.[42] As crystal-bound thiols are part of the anion sublattice of the Cu_2S, the cations still have access to the solution. The combination of robust ligand binding with open surface cation sites on particles with crystal-bound thiols may have important implications for the development of stable nanocrystal catalysts.

During the hydrolysis an additional insoluble black precipitate often formed. The precipitate was determined to be a CuO impurity by X-ray diffraction (XRD) (Supporting Information). It has been shown previously that Cu^{2+} ions leached from the oxidation of Cu_2S in the presence of a base and a surfactant can form CuO,[43,44] and the dodecanol liberated during the ester hydrolysis is capable of performing this function. However, the Cu_2S is only a small source of the copper ions that form CuO, as there was a negligible size change after the hydrolysis and a minimal change in stoichiometry from Cu_2S to $Cu_{1.98}S$. Therefore, we attribute the formation of the CuO from the presence of a copper impurity remaining from the synthesis that is especially difficult to remove from the nanocrystals when the nanocrystals are capped with D3MP.

Cu_2S is the parent structure of a large family of mixed cation copper sulfides including copper indium sulfide, copper gallium sulfide, copper indium gallium sulfide, and copper zinc tin sulfide.[45] The wide range of compositions of the mixed copper sulfides allows for tunable optical and electronic properties and have been extensively researched for energy-related applications. Nanocrystals of these materials, like those of Cu_2S, can be synthesized using thiols as a sulfur source to obtain high-quality products.[11,14−16] To demonstrate the broader applicability of our approach toward preparing water-soluble nanocrystals with crystal-bound thiols, $CuInS_2$ was synthesized[11] using D3MP. Copper and indium salts were heated in neat D3MP (Figure 8A), resulting in 2.41 ± 0.29 nm (n = 132) nanocrystals. The phase was confirmed to be chalcopyrite $CuInS_2$ by SAED and the stoichiometry $Cu_{1.2}In_{1.2}S_2$ by energy dispersive spectroscopy (EDS). The nanocrystals were subjected to the same hydrolysis procedure as the Cu_2S to give water-soluble $CuInS_2$ (Figure 8B). SAED confirmed the phase remained chalcopyrite $CuInS_2$ (Supporting Information) and the size was not significantly altered (2.34 ± 0.27 nm, n = 140). As in Cu_2S, the

phase transfer caused the formation of a surface plasmon resonance in the absorbance spectrum of the $CuInS_2$ (Figure 8C), which is known to be accompanied by a blue shift in the band gap, which is also observed.[46] The carrier density was calculated to be 1.44×10^{-21} cm^{-1}, the final stoichiometry was determined by quantitative EDS to be $Cu_{0.77}In_{0.90}S_{2.00}$ (Supporting Information), and the phase was confirmed by SAED to remain chalcopyrite $CuInS_2$. Currently, we are developing milder hydrolysis procedures to aid in the phase transfer of these highly sensitive materials without the changes in stoichiometry and optical properties.

CONCLUSION

Previous attempts at rendering nanocrystals prepared with thiols as the sulfur precursors water-soluble through ligand exchange were often ineffective. ^{1}H NMR, XPS, and TGA-MS reveal the surface chemistry is different between "surface-bound" ligands and "crystal-bound" ligands produced when thiols are used as sulfur sources. We explain the inert surfaces and more tightly bound ligands as a result of the sulfur atom of the thiol capping ligand being bound into a higher coordination site in the crystal lattice.

Previously, Wang *et al.* hinted at the possibility of high coordination number binding of thiols in a figure in their report of a similar synthesis of Cu_2S, but did not fully characterize or discuss this assignment.[47] We believe this is the first thorough description of the unique crystal-bound binding mode this synthetic route affords. Our description of this high coordination number binding mode of thiols on a nanocrystal surface is reminiscent of the "stapling" that has unambiguously been identified on thiolated gold clusters by X-ray crystal structure analysis.[48] In the staples, Au atoms are removed from the Au cluster surface to so that the thiolates have a gold coordination number of two. The decomposition of thiols on metal atoms to give metal sulfide nanocrystals has been well established for Cu,[49] Pd,[50] and Ni,[51] and it is possible that high coordination number binding of thiols also occurs in these cases.

To allow these high-quality particles with crystal-bound thiols to be rendered water-soluble, a new, easily synthesized ligand, dodecyl-3-mercaptopropanoate, can be used as a replacement for alkanethiols in the synthesis of copper(I) sulfide and copper indium sulfide. The ester functionality was hydrolyzed, yielding nanocrystals with a corona of carboxylic acids, which makes them soluble in water. The ester also provides a chemical handle for further surface functionalization, for example, amide coupling, which is a current topic of interest in our laboratory.[52]

EXPERIMENTAL SECTION

Materials. Sulfur (reagent grade), 1-dodecanol (98%), 3-mercaptopropanoic acid (>99%), oleylamine (70%), oleic acid (90%), dodecanethiol (97%), and dioctyl ether (99%) were obtained from Sigma-Aldrich. Copper(II) acetylacetonate (97%) was obtained from Strem Chemicals. Indium(III) acetate (99%) was obtained from Alfa Aesar. All chemical were used as obtained without further purification. Standard air-free Schlenk techniques were used throughout with N_2 used as the inert gas. The glovebox used was also filled with N_2.

Copper(I) Sulfide Nanocrystals with Crystal-Bound Ligands. Cu_2S was prepared following a modified literature procedure.[6] In a typical synthesis, $Cu(acac)_2$ (87.2 mg, 0.333 mmol) was dissolved in 2 mL of dodecanethiol and 8 mL of dioctyl ether and placed under vacuum for 1 h. The solution was heated to 200 °C under nitrogen. At 125 °C, the solution turned a transparent yellow color, and as the solution heated further, it became orange, signifying the formation of the Cu-thiol complex. At 200 °C the solution turned black, indicative of particle formation. The solution was reacted for 60 min at 200 °C, then allowed to cool to room temperature under nitrogen. The reaction flask was then brought into a glovebox to be washed. The particles were isolated by the addition of ethanol followed by centrifugation. The supernatant was removed, and the particles were suspended in chloroform and precipitated with ethanol three times. The final product was stored in a glovebox to prevent oxidation to a substoichiometric copper sulfide.

Copper(I) Sulfide with Surface-Bound Ligands. Cu_2S was prepared following a modified literature procedure.[26] In a typical synthesis $Cu(acac)_2$ (261 mg, 1.00 mmol) was dissolved in 10 mL of oleylamine and 5 mL of oleic acid and placed under vacuum for 1 h. The solution was then heated to 200 °C under nitrogen. At 200 °C, sulfur (16.0 mg 0.500 mmol) dissolved in 1 mL of oleylamine was quickly injected. The reaction was allowed to proceed for 30 min. The solution was cooled to room temperature and brought into a glovebox for washing. The resulting product was isolated by the addition of ethanol followed by centrifugation. The particles were then washed using chloroform and ethanol three times. The final product was stored in a glovebox to prevent oxidation to a substoichiometric copper sulfide.

Ligand Exchange of the Native Acid and Amine Ligands to Surface-Bound Thiols. Cu_2S with surface-bound ligands was dissolved in a minimum amount of chloroform. To 1 mL of the saturated solution of Cu_2S nanocrystals was added 0.5 mL of dodecanethiol. The solution was stirred at room temperature for 15 min in a glovebox. The particles were isolated by the addition of ethanol followed by centrifugation. The supernatant was removed, and the particles were suspended in chloroform and precipitated with ethanol two times. The final product was stored in a glovebox to prevent oxidation to a substoichiometric copper sulfide.

^{1}H NMR. ^{1}H NMR spectra of the nanoparticle solutions were acquired using a 11.7 T magnet equipped with a Bruker DRX console operating at 500.13 MHz. Chemical shifts were referenced internally to $CDCl_3$ (7.26 ppm), which also served as the ^{2}H lock solvent, and a delay time of 2 s was used. For the dynamic studies 1,2-dibromoethane was used as an internal standard for determination of the concentration of ligands present as part of the nanocrystal solution. The concentration was determined by comparing the integrations of the 1,2-dibromoethane peak at 3.65 ppm and the terminal $-CH_3$ group of the ligand at 0.88 ppm. The concentration of ligands in solution was around 1 mM. A solution of D3MP in $CDCl_3$ was then added to the NMR tube such that the molar amount of free ligand was equal to twice that of the bound ligand. The sample was then left for 24 h in ambient light.

X-ray Photoelectron Spectroscopy. The samples were prepared in a glovebox, and ^{1}H NMR in $CDCl_3$ confirmed there were ligands attached to the nanocrystals and that there were no residual

free ligands present. The nanocrystals were then drop cast from a suspension in $CHCl_3$ onto a silicon wafer. XPS was performed using a Physical Electronics (PHI) VersaProbe 5000. The data were collected using Al Kα X-rays (1486 eV), a takeoff angle of 45°, and a spot size of 100 μm. Peaks were fitted using CasaXPS software, calibrated to the lowest energy C 1s peak at 284.8 eV. In the S 2p spectra, the separation of the spin−orbit couple was set to 1.15 eV and the peak areas fixed to a ratio of 2:1. The fwhm's were constrained such that the spin−orbit couples had matching fwhm's but were otherwise allowed to fit freely. The fwhm's were between 0.99 and 1.19 eV.

Thermogravametric Analysis−Mass Spectrometry. ^{1}H NMR in $CDCl_3$ of the nanocrystals confirmed there were ligands attached to the nanocrystals and that there was no residual free ligands present. Analysis was performed on a PerkinElmer TL-2000 hyphenated TGA-GC-MS thermal analysis system. The GC column was a PerkinElmer Elite-5 (5% diphenyl) dimethylpolysiloxane series capillary column with 0.25 mm inner diameter. Helium is used as the carrier gas at a flow rate of 1 mL/min. Samples were thermalyzed using a PerkinElmer Pyris 1 TGA system. Sampling of the TGA oven atmosphere was controlled by a pneumatic Swafer valve system within the Clarus 680 GC instrument, and the evolved gases were transported through a deactivated silica capillary to the head of the GC column. The capillary transport line was heated isothermally at 200 °C for the duration of the experiment. Samples were loaded onto the GC column at regular intervals during the thermolysis. The evolved gases were generated, separated, and analyzed using MS under the following conditions: Splitless injection of gases onto the GC column was done at 200 °C as drawn from the TGA. GC oven temperature was keep isothermal at 250 °C for the duration of the run. Total ion count was recorded by the Clarus SQ 8C MS for the range $50 < m/z < 300$. The TGA was run using ∼10−20 mg of sample in Pt pans. The TGA oven was purged with helium at a rate of 100 mL/min during the run. TGA samples were held isothermally for 4 min at 50 °C and ramped at 10 °C/min until 900 °C.

Dodecyl 3-Mercaptopropanoate. Dodecyl 3-mercaptoproponate was prepared by a modified literature procedure.[39] In a typical synthesis, 1-dodecanol (22.0 g, 0.120 mol, 1.33 equiv) and 3-mercaptopropionic acid (7.50 mL 0.0900 mol, 1.00 equiv) were dissolved in 15 mL of toluene with 4 drops of concentrated H_2SO_4. The flask was fitted with a Dean−Stark trap filled with saturated aqueous KCl. The reagents were heated to reflux for 1 h. The resulting product was washed two times with 20 mL of brine followed by 20 mL of DI water. The organic layer was dried over $MgSO_4$, and the product purified by vacuum distillation (140 °C at 400 mTorr). Yield: 14 g (59%). ^{1}H NMR (400 MHz, $CDCl_3$): δ 4.10 (t, J = 6.72 Hz 2H, $-CO_2CH_2-$), 2.77 (q, J = 8.4 Hz, 2H, $-CH_2SH$), 2.65 (t, J = 6.9 Hz, 2H, $-CH_2CO_2-$), 1.63 (m, 3H, $-CO_2CH_2CH_2-$, $-SH$), 1.35−1.23 (m, 18H, $-CH_2-$ ×9), 0.88 (t, J = 7 Hz, 3H, $-CH_3$).

Copper(I) Sulfide Nanocrystals with Crystal-Bound D3MP. Cu_2S was prepared following a similar procedure to the Cu_2S with crystal-bound ligands used previously. In a typical synthesis, $Cu(acac)_2$ (87.2 mg, 0.333 mmol) was dissolved in 5 mL of D3MP and placed under vacuum for 1 h. The solution was heated to 200 °C under nitrogen. At 125 °C, the solution turned a transparent yellow color, and as the solution heated further, it became orange, signifying the formation of the Cu-thiol complex. At 200 °C the solution turned black, indicative of particle formation. The solution was reacted for 60 min at 200 °C, then was allowed to cool to room temperature under nitrogen. The flask was brought into a glovebox, where it was filled with 2-propanol. The particles were left to settle out of solution for 16 h. The 2-propanol was then removed, leaving a black solid. The particles were washed two times with 2-propanol then two times with chloroform in a glovebox, allowing for each precipitation step to be at least 16 h. The resulting solid was then stored in a glovebox as a suspension in $CHCl_3$.

Copper Indium Sulfide Nanocrystals. $CuInS_2$ was prepared following a modified literature procedure.[11] In a typical synthesis, $Cu(acac)_2$ (265.0 mg, 1 mmol) and $In(acac)_3$ (292.0 mg, 1 mmol) were combined in 5.00 mL of D3MP. The reaction was placed under vacuum for 1 h, then heated to 100 °C under nitrogen for 10 min to fully dissolve all the precursors. Upon heating to 230 °C, the solution changed from a transparent yellow to orange and finally black at 230 °C. The temperature was maintained for 1 h. The particles were isolated by adding 2-propanol followed by centrifugation. The supernatant was removed, and the resulting solid was suspended in hexanes and precipitated with 2-propanol two times.

Hydrolysis of D3MP-Capped Cu_2S and $CuInS_2$. Dried Cu_2S or $CuInS_2$ was obtained by removing the solvent under vacuum. The particles were then dissolved in a minimal amount of THF; typically 1−2 mL was needed. To the THF/Cu_2S solution was added an aqueous 0.1 M KOH solution in an amount equal to half the volume of THF used. The solution was stirred in a 50 °C water bath for 2 h. The particles were isolated by centrifuging the solution for 5 min at 4400 rpm. The precipitate was washed with ethanol and centrifuged for 5 min at 4400 rpm two times. The particles were then dispersed in water. The final aqueous solution was then centrifuged for 1 min at 1000 rpm. The precipitate was discarded and the supernatant collected.

Conflict of Interest: The authors declare no competing financial interest.

Supporting Information Available: Synthesis and ^{1}H NMR of the disulfides. Infrared spectrum of surface-bound ligands before and after exchange, full ^{1}H NMR spectra of Cu_2S with crystal-bound and surface-bound ligands, XRD of Cu_2S used for crystal-bound and surface-bound comparison, XPS Cu 2p regions, mass spectra from TGA-MS, SAED of particles before and after hydrolysis, absorbance of water-soluble particles extended into the near-IR, XRD of CuO impurity, and free carrier density calculations. This material is available free of charge *via* the Internet at http://pubs.acs.org.

Acknowledgment. We gratefully acknowledge the funding of this project by NSF-1253105 and NSF EPS-1004083 and the Vanderbilt Institute of Nanoscale Science and Engineering (VINSE). Additionally, M.J.T. would like to thank the Mitchum E. Warren fellowship. We would also like to thank Donald Stec of Vanderbilt University for his help with the NMR studies, Benjamin Schmidt of Vanderbilt University for his help with the XPS, and Jeffrey McDowell and Edward Sargent of University of Toronto for their help in collecting the TGA-MS data.

REFERENCES AND NOTES

1. Medintz, I. L.; Uyeda, H. T.; Goldman, E. R.; Mattoussi, H. Quantum Dot Bioconjugates for Imaging, Labelling and Sensing. *Nat. Mater.* **2005**, *4*, 435–446.
2. Talapin, D. V.; Lee, J. S.; Kovalenko, M. V.; Shevchenko, E. V. Prospects of Colloidal Nanocrystals for Electronic and Optoelectronic Applications. *Chem. Rev.* **2010**, *110*, 389–458.
3. Chen, X. B.; Li, C.; Gratzel, M.; Kostecki, R.; Mao, S. S. Nanomaterials for Renewable Energy Production and Storage. *Chem. Soc. Rev.* **2012**, *41*, 7909–7937.
4. Park, J.; Joo, J.; Kwon, S. G.; Jang, Y.; Hyeon, T. Synthesis of Monodisperse Spherical Nanocrystals. *Angew. Chem., Int. Ed.* **2007**, *46*, 4630–4660.
5. Green, M. The Nature of Quantum Dot Capping Ligands. *J. Mater. Chem.* **2010**, *20*, 5797–5809.
6. Choi, S. H.; An, K.; Kim, E. G.; Yu, J. H.; Kim, J. H.; Hyeon, T. Simple and Generalized Synthesis of Semiconducting Metal Sulfide Nanocrystals. *Adv. Funct. Mater.* **2009**, *19*, 1645–1649.
7. Sigman, M. B.; Ghezelbash, A.; Hanrath, T.; Saunders, A. E.; Lee, F.; Korgel, B. A. Solventless Synthesis of Monodisperse Cu_2S Nanorods, Nanodisks, and Nanoplatelets. *J. Am. Chem. Soc.* **2003**, *125*, 16050–16057.
8. Kuzuya, T.; Yamamuro, S.; Hihara, T.; Sumiyama, K. Water-Free Solution Synthesis of Monodisperse Cu_2S Nanocrystals. *Chem. Lett.* **2004**, *33*, 352–353.
9. Zhuang, Z. B.; Peng, Q.; Zhang, B.; Li, Y. D. Controllable Synthesis of Cu_2S Nanocrystals and Their Assembly into a Superlattice. *J. Am. Chem. Soc.* **2008**, *130*, 10482–10483.

10. Kruszynska, M.; Borchert, H.; Bachmatiuk, A.; Rummeli, M. H.; Buchner, B.; Parisi, J.; Kolny-Olesiak, J. Size and Shape Control of Colloidal Copper(I) Sulfide Nanorods. *ACS Nano* **2012**, *6*, 5889–5896.
11. Li, L. A.; Pandey, A.; Werder, D. J.; Khanal, B. P.; Pietryga, J. M.; Klimov, V. I. Efficient Synthesis of Highly Luminescent Copper Indium Sulfide-Based Core/Shell Nanocrystals with Surprisingly Long-Lived Emission. *J. Am. Chem. Soc.* **2011**, *133*, 1176–1179.
12. Kruszynska, M.; Borchert, H.; Parisi, J.; Kolny-Olesiak, J. Synthesis and Shape Control of $CuInS_2$ Nanoparticles. *J. Am. Chem. Soc.* **2010**, *132*, 15976–15986.
13. Xie, R. G.; Rutherford, M.; Peng, X. G. Formation of High-Quality I-III-VI Semiconductor Nanocrystals by Tuning Relative Reactivity of Cationic Precursors. *J. Am. Chem. Soc.* **2009**, *131*, 5691–5697.
14. Wang, Y. H. A.; Zhang, X. Y.; Bao, N. Z.; Lin, B. P.; Gupta, A. Synthesis of Shape-Controlled Monodisperse Wurtzite $CuIn_XGa_{1-X}S_2$ Semiconductor Nanocrystals with Tunable Band Gap. *J. Am. Chem. Soc.* **2011**, *133*, 11072–11075.
15. Singh, A.; Geaney, H.; Laffir, F.; Ryan, K. M. Colloidal Synthesis of Wurtzite Cu_2ZnSnS_4 Nanorods and Their Perpendicular Assembly. *J. Am. Chem. Soc.* **2012**, *134*, 2910–2913.
16. Han, W.; Yi, L. X.; Zhao, N.; Tang, A. W.; Gao, M. Y.; Tang, Z. Y. Synthesis and Shape-Tailoring of Copper Sulfide/Indium Sulfide-Based Nanocrystals. *J. Am. Chem. Soc.* **2008**, *130*, 13152–13161.
17. Jun, S.; Jang, E. Bright and Stable Alloy Core/Multishell Quantum Dots. *Angew. Chem., Int. Ed.* **2013**, *52*, 679–682.
18. Jun, S.; Jang, E. J.; Chung, Y. S. Alkyl Thiols as a Sulfur Precursor for the Preparation of Monodisperse Metal Sulfide Nanostructures. *Nanotechnology* **2006**, *17*, 4806–4810.
19. Chen, O.; Zhao, J.; Chauhan, V. P.; Cui, J.; Wong, C.; Harris, D. K.; Wei, H.; Han, H. S.; Fukumura, D.; Jain, R. K.; *et al*. Compact High-Quality CdSe-CdS Core-Shell Nanocrystals with Narrow Emission Linewidths and Suppressed Blinking. *Nat. Mater.* **2013**, *12*, 445–451.
20. Bae, W. K.; Padilha, L. A.; Park, Y. S.; McDaniel, H.; Robel, I.; Pietryga, J. M.; Klimov, V. I. Controlled Alloying of the Core-Shell Interface in CdSe/CdS Quantum Dots for Suppression of Auger Recombination. *ACS Nano* **2013**, *7*, 3411–3419.
21. Bryks, W.; Wette, M.; Velez, N.; Hsu, S.-W.; Tao, A. R. Supramolecular Precursors for the Synthesis of Anisotropic Cu_2S Nanocrystals. *J. Am. Chem. Soc.* **2014**, *136*, 6175–6178.
22. Vinokurov, K.; Macdonald, J. E.; Banin, U. Structures and Mechanisms in the Growth of Hybrid Ru-Cu_2S Nanoparticles: From Cages to Nanonets. *Chem. Mater.* **2012**, *24*, 1822–1827.
23. Luther, J. M.; Law, M.; Song, Q.; Perkins, C. L.; Beard, M. C.; Nozik, A. J. Structural, Optical and Electrical Properties of Self-Assembled Films of PbSe Nanocrystals Treated with 1,2-Ethanedithiol. *ACS Nano* **2008**, *2*, 271–280.
24. Owen, J. S.; Park, J.; Trudeau, P. E.; Alivisatos, A. P. Reaction Chemistry and Ligand Exchange at Cadmium-Selenide Nanocrystal Surfaces. *J. Am. Chem. Soc.* **2008**, *130*, 12279–12281.
25. Anderson, N. C.; Hendrix, M. P.; Choi, J. J.; Owen, J. S. Ligand Exchange and the Stoichiometry of Metal Chalcogenide Nanocrystals: Spectroscopic Observation of Facile Metal-Carboxylate Displacement and Binding. *J. Am. Chem. Soc.* **2013**, *135*, 18536–18548.
26. Kim, Y.; Park, K. Y.; Jang, D. M.; Song, Y. M.; Kim, H. S.; Cho, Y. J.; Myung, Y.; Park, J. Synthesis of Au-Cu_2S Core-Shell Nanocrystals and Their Photocatalytic and Electrocatalytic Activity. *J. Phys. Chem. C* **2010**, *114*, 22141–22146.
27. Fritzinger, B.; Capek, R. K.; Lambert, K.; Martins, J. C.; Hens, Z. Utilizing Self-Exchange to Address the Binding of Carboxylic Acid Ligands to CdSe Quantum Dots. *J. Am. Chem. Soc.* **2010**, *132*, 10195–10201.
28. Moreels, I.; Martins, J. C.; Hens, Z. Ligand Adsorption/Desorption on Sterically Stabilized InP Colloidal Nanocrystals: Observation and Thermodynamic Analysis. *ChemPhysChem* **2006**, *7*, 1028–1031.
29. Hens, Z.; Martins, J. C. A Solution NMR Toolbox for Characterizing the Surface Chemistry of Colloidal Nanocrystals. *Chem. Mater.* **2013**, *25*, 1211–1221.
30. Gomes, R.; Hassinen, A.; Szczygiel, A.; Zhao, Q. A.; Vantomme, A.; Martins, J. C.; Hens, Z. Binding of Phosphonic Acids to CdSe Quantum Dots: A Solution NMR Study. *J. Phys. Chem. Lett.* **2011**, *2*, 145–152.
31. Nørby, P.; Johnsen, S.; Iversen, B. B. In Situ X-Ray Diffraction Study of the Formation, Growth, and Phase Transition of Colloidal $Cu_{2-X}S$ Nanocrystals. *ACS Nano* **2014**, *8*, 4295–4303.
32. Aldana, J.; Wang, Y. A.; Peng, X. G. Photochemical Instability of CdSe Nanocrystals Coated by Hydrophilic Thiols. *J. Am. Chem. Soc.* **2001**, *123*, 8844–8850.
33. Li, X. B.; Li, Z. J.; Gao, Y. J.; Meng, Q. Y.; Yu, S.; Weiss, R. G.; Tung, C. H.; Wu, L. Z. Mechanistic Insights into the Interface-Directed Transformation of Thiols into Disulfides and Molecular Hydrogenby Visible-Light Irradiation of Quantum Dots. *Angew. Chem., Int. Ed.* **2014**, *53*, 2085–2089.
34. Xie, Y.; Riedinger, A.; Prato, M.; Casu, A.; Genovese, A.; Guardia, P.; Sottini, S.; Sangregorio, C.; Miszta, K.; Ghosh, S.; *et al*. Copper Sulfide Nanocrystals with Tunable Composition by Reduction of Covellite Nanocrystals with Cu^+ Ions. *J. Am. Chem. Soc.* **2013**, *135*, 17630–17637.
35. Li, H. B.; Brescia, R.; Povia, M.; Prato, M.; Bertoni, G.; Manna, L.; Moreels, I. Synthesis of Uniform Disk-Shaped Copper Telluride Nanocrystals and Cation Exchange to Cadmium Telluride Quantum Disks with Stable Red Emission. *J. Am. Chem. Soc.* **2013**, *135*, 12270–12278.
36. Lai, Y. H.; Yeh, C. T.; Cheng, S. H.; Liao, P.; Hung, W. H. Adsorption and Thermal Decomposition of Alkanethiols on Cu(110). *J. Phys. Chem. B* **2002**, *106*, 5438–5446.
37. Berkowitz, J.; Marquart, J. R. Equilibrium Composition of Sulfur Vapor. *J. Chem. Phys.* **1963**, *39*, 275–283.
38. de Petris, G.; Cartoni, A.; Rosi, M.; Troiani, A. The HSSS Radical and the $HSSS^-$ Anion. *J. Phys. Chem. A* **2008**, *112*, 8471–8477.
39. Byrne, C.; Sallas, F.; Rai, D. K.; Ogier, J.; Darcy, R. Poly-6-Cationic Amphiphilic Cyclodextrins Designed for Gene Delivery. *Org. Biomol Chem.* **2009**, *7*, 3763–3771.
40. Zhao, Y. X.; Pan, H. C.; Lou, Y. B.; Qiu, X. F.; Zhu, J. J.; Burda, C. Plasmonic $Cu_{2-X}S$ Nanocrystals: Optical and Structural Properties of Copper-Deficient Copper(I) Sulfides. *J. Am. Chem. Soc.* **2009**, *131*, 4253–4261.
41. Luther, J. M.; Jain, P. K.; Ewers, T.; Alivisatos, A. P. Localized Surface Plasmon Resonances Arising from Free Carriers in Doped Quantum Dots. *Nat. Mater.* **2011**, *10*, 361–366.
42. Macdonald, J. E.; Bar Sadan, M.; Houben, L.; Popov, I.; Banin, U. Hybrid Nanoscale Inorganic Cages. *Nat. Mater.* **2010**, *9*, 810–815.
43. Wen, X. G.; Zhang, W. X.; Yang, S. H. Solution Phase Synthesis of $Cu(OH)_2$ Nanoribbons by Coordination Self-Assembly Using Cu2s Nanowires as Precursors. *Nano Lett.* **2002**, *2*, 1397–1401.
44. Wang, W. Z.; Zhou, Q.; Fei, X. M.; He, Y. B.; Zhang, P. C.; Zhang, G. L.; Peng, L.; Xie, W. J. Synthesis of CuO Nano- and Micro-Structures and Their Raman Spectroscopic Studies. *CrystEngComm* **2010**, *12*, 2232–2237.
45. Zhao, Y. X.; Burda, C. Development of Plasmonic Semiconductor Nanomaterials with Copper Chalcogenides for a Future with Sustainable Energy Materials. *Energy Environ. Sci.* **2012**, *5*, 5564–5576.
46. Niezgoda, J. S.; Harrison, M. A.; McBride, J. R.; Rosenthal, S. J. Novel Synthesis of Chalcopyrite $Cu_xIn_yS_2$ Quantum Dots with Tunable Localized Surface Plasmon Resonances. *Chem. Mater.* **2012**, *24*, 3294–3297.
47. Tang, A. W.; Qu, S. C.; Li, K.; Hou, Y. B.; Teng, F.; Cao, J.; Wang, Y. S.; Wang, Z. G. One-Pot Synthesis and Self-Assembly of Colloidal Copper(I) Sulfide Nanocrystals. *Nanotechnology* **2010**, 21.
48. Jadzinsky, P. D.; Calero, G.; Ackerson, C. J.; Bushnell, D. A.; Kornberg, R. D. Structure of a Thiol Monolayer-Protected Gold Nanoparticle at 1.1 Angstrom Resolution. *Science* **2007**, *318*, 430–433.

49. Mott, D.; Yin, J.; Engelhard, M.; Loukrakpam, R.; Chang, P.; Miller, G.; Bae, I. T.; Das, N. C.; Wang, C. M.; Luo, J.; *et al*. From Ultrafine Thiolate-Capped Copper Nanoclusters toward Copper Sulfide Nanodiscs: A Thermally Activated Evolution Route. *Chem. Mater.* **2010**, *22*, 261–271.
50. Corthey, G.; Rubert, A. A.; Picone, A. L.; Casillas, G.; Giovanetti, L. J.; Ramallo-Lopez, J. M.; Zelaya, E.; Benitez, G. A.; Requejo, F. G.; Jose-Yacaman, M.; *et al*. New Insights into the Chemistry of Thiolate-Protected Palladium Nanoparticles. *J. Phys. Chem. C* **2012**, *116*, 9830–9837.
51. Calderon, M. F.; Zelaya, E.; Benitez, G. A.; Schilardi, P. L.; Creus, A. H.; Orive, A. G.; Salvarezza, R. C.; Ibanez, F. J. New Findings for the Composition and Structure of Ni Nanoparticles Protected with Organomercaptan Molecules. *Langmuir* **2013**, *29*, 4670–4678.
52. Sperling, R. A.; Parak, W. J. Surface Modification, Functionalization and Bioconjugation of Colloidal Inorganic Nanoparticles. *Philos. Trans. R. Soc. A* **2010**, *368*, 1333–1383.